Electronic Supplementary Material (ESI) for Catalysis Science & Technology.

Methanol reforming denitration over integrated bifunctional $CuZnO_x$-X-$MnPdO_z$@Ni catalyst at low temperature

Tianying Xie [a], Limei Cao [a], Wei Sun[b], Ji Yang[, a,c]*

[a]School of Resources and Environmental Engineering, State Environmental Protection Key Laboratory of Environmental Risk Assessment and Control on Chemical Process, East China University of Science and Technology, Shanghai 200237, P.R. China

[b]College of Ecology and Environment, Hainan University, 58 Renmin Road, Haikou 570228, P.R. China

[c]Shanghai Institute of Pollution Control and Ecological Security, Shanghai200092, P.R.China

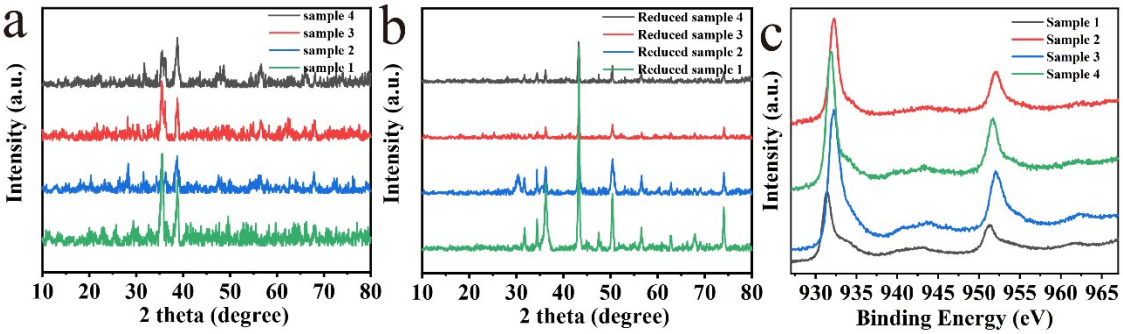

Figure. S1 (a)(b)The XRD images of $CuZnO_x$-X-$MnPdO_z$ catalyst（1-4 represented $CuZnO_x$-AlO_y-$MnPdO_z$, $CuZnO_x$-CeO_y-$MnPdO_z$, $CuZnO_x$-ZrO_y-$MnPdO_z$, $CuZnO_x$-$CeZrO_y$-$MnPdO_z$, respectively (c) XPS pattern of $CuZnO_x$-X-$MnPdO_z$ catalyst

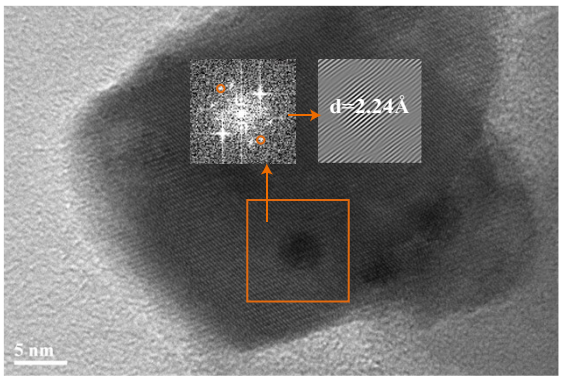

Figure. S2 The TEM images of $CuZnO_x$-X-$MnPdO_z$ catalyst

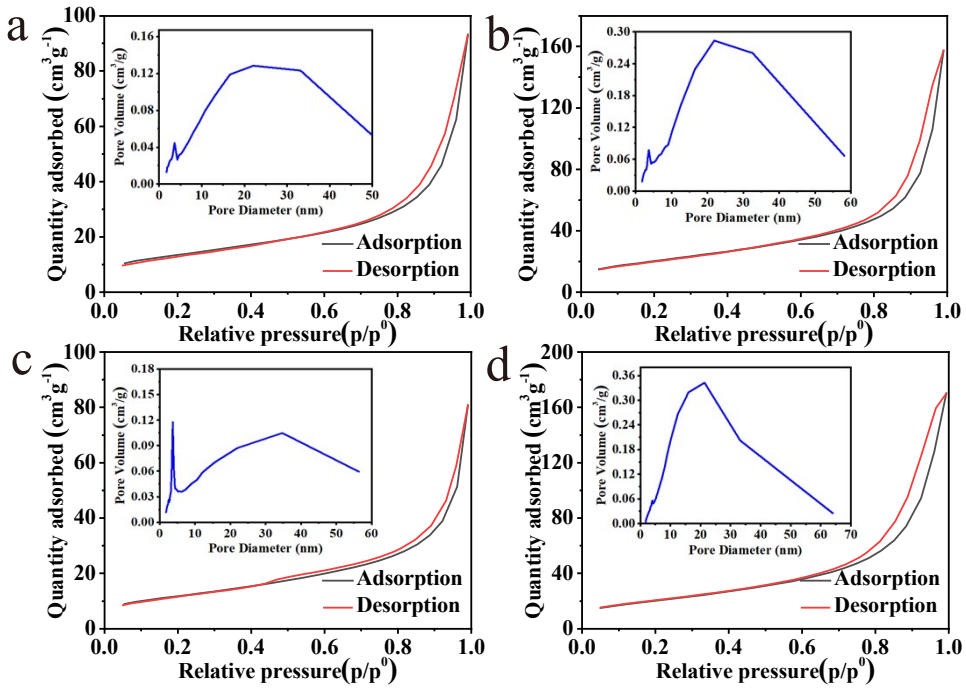

Figure. S3 The Nitrogen adsorption-desorption curves of $CuZnO_x$-X-$MnPdO_z$ catalyst

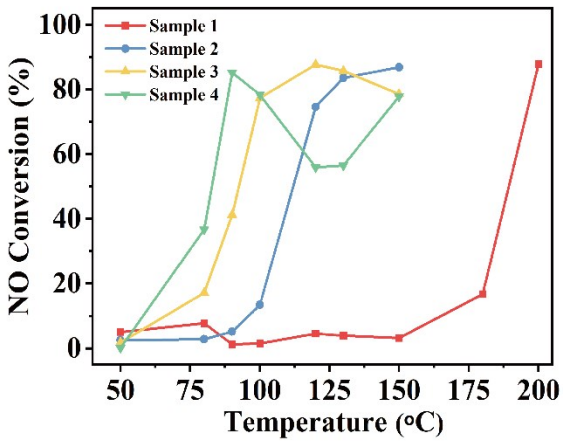

Figure. S4 H_2-SCR performance of prepared catalyst, sample 1-4 represented 0.08%, 0.25%, 0.42% Pd doped MnNiOx catalyst, and $CuZnO_x$-CeZrOy-$MnPdO_z$ catalyst

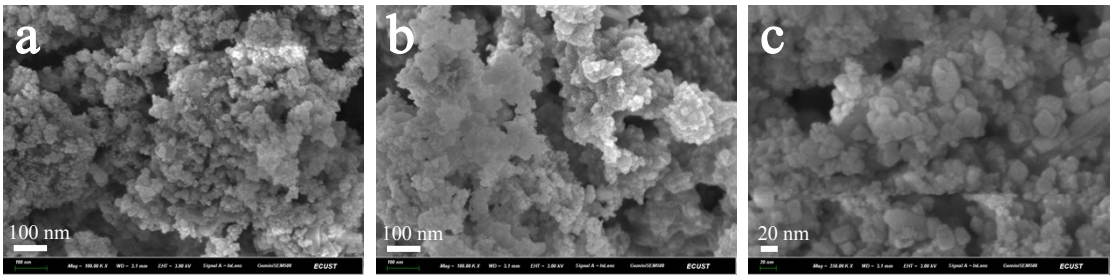

Figure. S5 The SEM images of $CuZnO_x$-X-$MnPdO_z$ catalyst

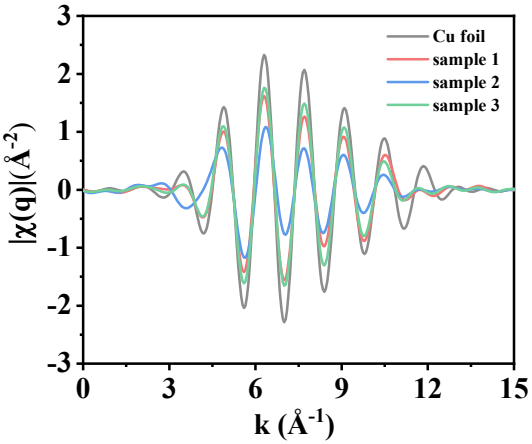

Figure. S6 The k^2-weighted EXAFS spectrum of $CuZnO_x$-X-$MnPdO_z$ catalyst (sample 1 represented $CuZnO_x$-$CeZrO_y$ @Ni, sample 2 represented $CuZnO_x$-$CeZrO_y$-$MnPd^1O_z$@Ni, sample 3 represented $CuZnO_x$-$CeZrO_y$-$MnPd^2O_z$@Ni, respectively; superscripts 1 and 2 represented 0.08% and 0.42%Pd contents)

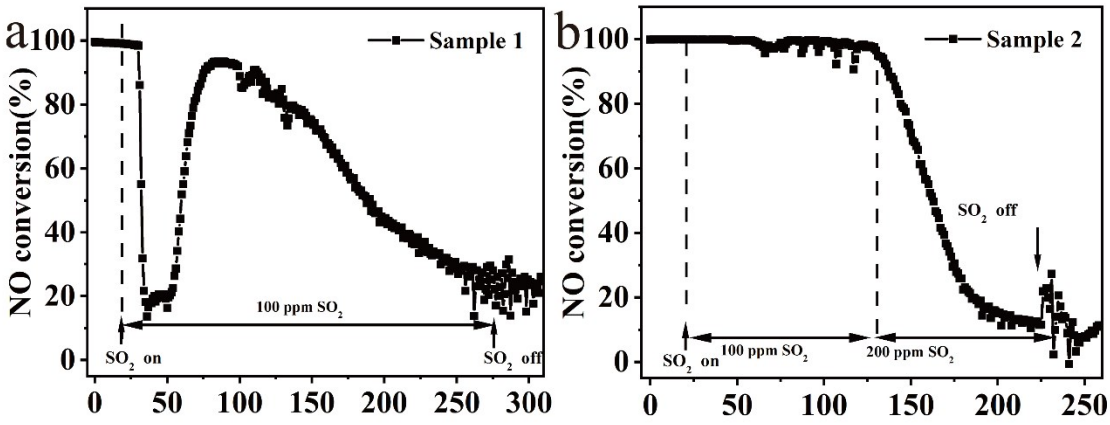

Figure. S7 sulfur-resistance of the $CuZnO_x$-X-$MnPdO_z$@Ni catalyst, sample 1 represented $CuZnO_x$-AlOy-$MnPdO_z$@Ni, sample 2 represented $CuZnO_x$-ZrOy-$MnPdO_z$@Ni